Toward a Robust Canopy Hydrology Scheme with Precipitation Subgrid Variability

DAGANG WANG AND GUILING WANG

Department of Civil and Environmental Engineering, University of Connecticut, Storrs, Connecticut

(Manuscript received 9 February 2006, in final form 28 September 2006)

ABSTRACT

Representation of the canopy hydrological processes has been challenging in land surface modeling due to the subgrid heterogeneity in both precipitation and surface characteristics. The Shuttleworth dynamic–statistical method is widely used to represent the impact of the precipitation subgrid variability on canopy hydrological processes but shows unwanted sensitivity to temporal resolution when implemented into land surface models. This paper presents a canopy hydrology scheme that is robust at different temporal resolutions. This scheme is devised by applying two physically based treatments to the Shuttleworth scheme: 1) the canopy hydrological processes within the rain-covered area are treated separately from those within the nonrain area, and the scheme tracks the relative rain location between adjacent time steps; and 2) within the rain-covered area, the canopy interception is so determined as to sustain the potential evaporation from the wetted canopy or is equal to precipitation, whichever is less, to maintain somewhat wet canopy during any rainy time step. When applied to the Amazon region, the new scheme establishes interception loss ratios of 0.3 at a 10-min time step and 0.23 at a 2-h time step. Compared to interception loss ratios of 0.45 and 0.09 at the corresponding time steps established by the original Shuttleworth scheme, the new scheme is much more stable under different temporal resolutions.

1. Introduction

Interception loss, the part of precipitation lost via evaporation from the wetted vegetation canopy, constitutes a significant portion of gross precipitation, especially over densely vegetated areas. Its value ranges from 12% to 48% of gross precipitation depending on the vegetation types, and the regional climate conditions (Hörmann et al. 1996). Rutter et al. (1971, 1975) developed a physically based model for characterizing canopy hydrological processes at a point scale. Gash (1979) and Gash et al. (1995) derived an analytical model of interception loss on the basis of the Rutter model. These two models have been widely used in different types of areas in which the interception losses from model simulations have reasonable agreements with observations.

Canopy interception plays an important role in land–atmosphere interactions. Scott et al. (1995) compared results from a model with a canopy interception reservoir and one without using a coupled land–atmosphere model and found that including interception loss reduced the persistence of precipitation and evapotranspiration anomalies. Its impact is stronger in densely vegetated areas, such as the Amazon basin. However, due to the significant subgrid land surface variability within a typical grid cell of the general circulation model (GCM) and the lack of global calibrated parameters for modeling, realistic representation of interception loss is more difficult in GCM than at a point scale. Using the Biosphere–Atmosphere Transfer Scheme (BATS) coupled with an atmosphere model, Dickinson and Henderson-Sellers (1988) found that the simulated interception loss over the Amazon basin is 150% higher than observed. Lean and Warrilow (1989) also reported significant overestimation of interception loss using the Met Office Model.

Shuttleworth (1988b) developed an interception scheme that incorporated the precipitation subgrid variability into the canopy hydrological processes. This scheme has been widely used to investigate the impact of the precipitation subgrid variability on surface hydrological processes (Pitman et al. 1990, 1993; Dolman and Gregory 1992; Wang and Eltahir 2000; Wang et al. 2005). Among these studies, Dolman and Gregory

Corresponding author address: Mr. Dagang Wang, Department of Civil and Environmental Engineering, University of Connecticut, 261 Glenbrook Rd., Storrs, CT 06269-2037.
E-mail: dagang.wang@uconn.edu

DOI: 10.1175/JHM585.1

(1992) reported that the effect of the precipitation subgrid variability is sensitive to the model time step when using the Shuttleworth (1988b) scheme. To avoid this sensitivity, they made the following adjustments: whatever the model time step is, the calculated canopy throughfall rate is taken as the hourly value; the total throughfall amount is then integrated over time; and, consequently, the actual throughfall rate is adjusted by the total amount over the model time step. In this note we propose a more physically based canopy hydrology scheme based on our previous work (Wang et al. 2005, hereafter W05) that uses the Shuttleworth scheme, which significantly reduces the temporal resolution sensitivity.

2. Toward a robust canopy hydrology scheme

The Shuttleworth (1988b) approach assumes that 1) rain falls over a fraction μ of the grid cell and follows a probability distribution $f(P)$ within the rain-covered area; 2) canopy dripping occurs only when the canopy storage exceeds its water holding capacity, and the excess storage is routed to the ground almost instantaneously; 3) what stays on the canopy is determined by the difference between the local rain-rate P and maximum canopy infiltration rate I_{max}; and 4) the canopy storage is uniformly redistributed across the whole grid cell at the end of each time step, and the difference between the canopy holding capacity and its grid-averaged storage is used to estimate I_{max} at the beginning of the next time step. Following this approach and the proposal of Eltahir and Bras (1993), W05 presents a study that makes use of high-resolution satellite rainfall observation in estimating μ and $f(P)$. The fraction μ is estimated as the ratio of the model-predicted rainfall intensity P_m to the conditional mean rainfall intensity P_o derived from high-resolution observational data, $\mu = P_m/P_o$, which varies temporally and spatially. Different probability density functions (pdfs) are used to represent the spatial distributions of different regions of interest. Further details can be found in W05.

When applying this data-enhanced scheme to the Community Land Model version 3 (CLM3), Wang et al. (2005) use a temporal resolution of 60 min, which is typical of land surface models running in their standalone mode. Later on when the model is run at different temporal resolutions (i.e., 10 min, 20 min, and 2 h), the results are dramatically different, as shown in section 3. It becomes clear that this scheme is highly sensitive to changes in temporal resolution, a problem also documented in other models that used the Shuttleworth approach (Dolman and Gregory 1992). We have identified two major causes for this undesirable model sensitivity. One operates more frequently when the temporal resolution is coarse and the other operates more frequently when the temporal resolution is fine.

At coarse temporal resolution, the problem is quite straightforward. When the time step is too long, even filling the canopy storage up to its holding capacity at the beginning of a rainy time step may not provide enough water to sustain continuous potential evaporation from the wetted canopy area throughout the time step. This implies that the canopy can be completely dry during part of a time step while it rains throughout the time step, which is not physically possible. To address this problem, during each rainy time step in the model after new interception is added to the canopy, we check whether the updated canopy water storage within the rain-covered area S_{rain} is enough to sustain a continuous potential evaporation from the wetted fraction of the canopy. When it is not, the partitioning of rain between canopy interception and throughfall will be adjusted so that S_{rain} equals the amount needed to sustain the potential evaporation from wetted canopy throughout the time step or equals the precipitation amount, whichever is less:

$$S_{\text{rain}}^{\text{adjusted}} = \max(\min(\text{fwet}_{\text{rain}} E_p \Delta t, P\Delta t), S_{\text{rain}}), \quad (1)$$

where $\text{fwet}_{\text{rain}}$ is the fraction of wetted canopy within the rain-covered area, E_p is the potential evaporation, Δt is the model time step, and P is the precipitation rate. Note that this adjustment increases the canopy interception at the expense of throughfall, so throughfall should be adjusted correspondingly.

At fine temporal resolution, it is the uniform redistribution of canopy water storage across each grid cell between different time steps that causes the problem of time step sensitivity. Due to this redistribution, the grid-averaged canopy storage is used to estimate the maximum infiltration rate I_{max} at the beginning of each time step. The smaller the canopy water storage, the larger I_{max}. When a convective storm occurs, it usually continues to rain within the same rain-covered area for quite a while. Consequently, within the typical rain duration (i.e., if rain does not shift location) the estimate of I_{max} should be based on the canopy water storage within the rainfall coverage fraction of a grid cell. When the model time step is smaller than the typical rain duration, I_{max} tends to be overestimated because uniformly redistributing the canopy water across each grid cell at the end of each time step leads to underestimate of the canopy water storage within the rain-covered area. Cosgrove (1999) studied the convective rain characteristics over the Florida peninsula that covers an area of 9430 km^2 and consists of 35 gauges. Based on the 65 convective rain events in July and August, it is found that the most frequent rain duration at a gauge site is between 50 and 60 min. Although the duration was observed in the Florida peninsula, these results have implications elsewhere. For a typical rain duration of approximately 1 h, if the model time step is less than 1 h, the uniform redistribution of canopy water between time steps will cause an overestimate of $I_{\max}$ and therefore an overestimate of the interception loss. The smaller the model time step is, the more frequently this bias occurs and the larger this bias becomes when averaged over time. To address this problem, we propose a scheme that treats canopy storage in the rain-covered area (S_{rain}) separately from that in the nonrain area (S_{norain}) and tracks the relative location of the rain between adjacent time steps in the current study, which differs from our previous study including averaged canopy storage across each grid cell at each time step.

Note that we assume the canopy dripping occurs only if the canopy water storage exceeds its holding capacity and the excessive storage is routed to canopy dripping instantaneously. Under this assumption, canopy dripping occurs within the rain-covered area only. Within the nonrain area, without replenishment from rain, the canopy water storage does not exceed its holding capacity after the previous dripping and evaporation. Therefore both interception rate and dripping rate are zero within the nonrain area. If precipitation within the rain-covered area follows an exponential distribution, what stays on the canopy can be estimated as

$$\begin{cases} \text{Ic}_{\text{rain}} - \text{Dr}_{\text{rain}} = \dfrac{P_m}{\mu} - \dfrac{P_m \exp\left(-\dfrac{\mu I_{\max}}{P_m}\right)}{\mu}, \\ \text{Ic}_{\text{norain}} = \text{Dr}_{\text{norain}} = 0 \end{cases} \quad (2)$$

where Ic_{rain} ($\text{Ic}_{\text{norain}}$) is the canopy interception rate within the rain-covered (nonrain) area, Dr_{rain} ($\text{Dr}_{\text{norain}}$) is the canopy dripping rate within the rain-covered (nonrain) area, P_m is grid-averaged precipitation intensity (simulated by the atmospheric model or derived from reanalysis data), and μ is the rainfall coverage fraction and estimated as P_m/P_o with conditional rain rate P_o derived from high-resolution observational data. The maximum canopy infiltration rate $I_{\max}$ in Eq. (2) is estimated based on the canopy storage at the beginning of the current time step within the rain-covered area (Sb_{rain}):

$$I_{\max} = \frac{C - \text{Sb}_{\text{rain}}}{\Delta t}, \quad (3)$$

where C is the canopy storing capacity. After interception, only the canopy water storage within the rain-covered area gets replenished from rainfall, while the storage within the nonrain area stays as it was. These different canopy water storages give rise to different wetted fractions of canopy and therefore different interception losses within these two types of areas.

What distinguishes this scheme from W05 is the use of beginning storage within the rain-covered area Sb_{rain} instead of the grid-averaged storage Sb_m in estimating $I_{\max}$, but quantifying Sb_{rain} requires tracking the relative locations of rain between adjacent time steps. Convective rain tends to stay over the same area for a certain period of time before shifting to other areas. To account for this fact, we assume a typical rain duration of 1h according to the Cosgrove (1999) study. The canopy water storage at the beginning of time step n (i.e., the beginning storage before new interception takes place) within the rain-covered area $\text{Sb}^n_{\text{rain}}$ and within the nonrain area $\text{Sb}^n_{\text{norain}}$ can be estimated based on theses storages at the end of the previous time step ($\text{Se}^{n-1}_{\text{rain}}$ and $\text{Se}^{n-1}_{\text{norain}}$) differently under different situations, as explained in the following:

(a) If it continues to rain during the current time step (n) over the same location as the previous time step, care is taken to maximize the overlapping of rain-covered areas between these two time steps:

$$\begin{cases} \text{Sb}^n_{\text{rain}} = \text{Se}^{n-1}_{\text{rain}} \dfrac{\mu^{n-1}}{\mu^n} + \text{Se}^{n-1}_{\text{norain}} \dfrac{\mu^n - \mu^{n-1}}{\mu^n} \\ \text{Sb}^n_{\text{norain}} = \text{Se}^{n-1}_{\text{norain}} \end{cases} \qquad \mu^n > \mu^{n-1} \quad \text{and} \quad (4)$$

$$\begin{cases} \text{Sb}^n_{\text{rain}} = \text{Se}^{n-1}_{\text{rain}} \\ \text{Sb}^n_{\text{norain}} = \text{Se}^{n-1}_{\text{rain}} \dfrac{\mu^{n-1} - \mu^n}{1 - \mu^n} + \text{Se}^{n-1}_{\text{norain}} \dfrac{1 - \mu^{n-1}}{1 - \mu^n} \end{cases} \qquad \mu^n < \mu^{n-1}. \quad (5)$$

(b) If rain shifts location from the previous time step to the current time step, care is taken to minimize the overlapping of rain-covered areas between these two time steps:

$$\begin{cases} \mathrm{Sb}^n_{\mathrm{rain}} = \mathrm{Se}^{n-1}_{\mathrm{norain}} \\ \mathrm{Sb}^n_{\mathrm{norain}} = \mathrm{Se}^{n-1}_{\mathrm{rain}} \dfrac{\mu^{n-1}}{1-\mu^n} + \mathrm{Se}^{n-1}_{\mathrm{norain}} \dfrac{1-\mu^{n-1}-\mu^n}{1-\mu^n} \end{cases} \qquad \mu^n + \mu^{n-1} < 1 \quad \text{and} \tag{6}$$

$$\begin{cases} \mathrm{Sb}^n_{\mathrm{rain}} = \mathrm{Se}^{n-1}_{\mathrm{rain}} \dfrac{\mu^n + \mu^{n-1} - 1}{\mu^n} + \mathrm{Se}^{n-1}_{\mathrm{norain}} \dfrac{1-\mu^{n-1}}{\mu^n} \\ S^n_{\mathrm{norain}} = S^{n-1}_{\mathrm{rain}} \end{cases} \qquad \mu^n + \mu^{n-1} > 1. \tag{7}$$

(c) If it does not rain during the current time step and it is the first time step after the rain stops, then the rainfall coverage fraction is zero, and both the $\mathrm{Sb}^n_{\mathrm{rain}}$ (kept for the use in future rainy time steps) and $\mathrm{Sb}^n_{\mathrm{norain}}$ are set to the grid-averaged canopy water storage:

$$\begin{aligned} \mathrm{Sb}^n_{\mathrm{rain}} &= \mathrm{Sb}^n_{\mathrm{norain}} \\ &= \mathrm{Se}^{n-1}_{\mathrm{rain}} \mu^{n-1} + \mathrm{Se}^{n-1}_{\mathrm{norain}} (1 - \mu^{n-1}). \end{aligned} \tag{8}$$

As such, the memory for water storage in the previous time step within the rain-covered and the nonrain areas is kept only during a continuous rain event. Once rain stops in that grid cell, this memory is lost. During the first time step when a new rain event starts, it can rain over any part of the grid cell.

The concept of dividing the grid cell into rain-covered and nonrain areas in the current study is similar to that in the Variable Infiltration Capacity (VIC) model (Liang et al. 1996) that considers impact of the rainfall subgrid variability on processes, such as interception, infiltration, and runoff. However, the current study is different than Liang et al. (1996) in determining the migration of the rain-covered area with time. The rainfall location changes only when the next rain event starts in VIC, while we use the convective rainfall duration at the site scale to track the relative rainfall location between adjacent time steps, namely, it continues to rain at the same location within a typical rainfall duration and the location changes beyond the duration. When a convective rain occurs, the passing time over a specific site is usually shorter than the lifetime of the whole storm event. We therefore consider it more appropriate to use rainfall duration at the site scale, instead of the rain duration for the whole storm event at the grid cell scale, to determine the rainfall location for convective rain.

3. Experiments' design and results

To examine the performance of this new scheme under different temporal resolutions, we carry out the simulations (EXP1) using CLM3 at the time steps of 10 min, 20 min, 1 h, and 2 h. The scheme in W05, which accounts for rainfall subgrid variability alone in the representation of canopy interception, is taken as a reference for the comparison. The difference between EXP1 and W05 is attributed to the two treatments: 1) adjusting the partition between canopy interception and throughfall to maintain a somewhat wet canopy during any rainy time step within the rain-covered area as described in Eq. (1); and 2) accounting for the subgrid variability of canopy storage and tracking the relative location of rain between adjacent time steps as described in Eqs. (2)–(8). To implore the relative importance of these two treatments in reducing the sensitivity to temporal resolution, we design two additional experiments: one (EXP2) is otherwise the same as EXP1 except excluding treatment 1; in contrast, the other (EXP3) is different than EXP1 in excluding treatment 2. In some of these experiments, the typical rain duration is needed to determine the relative rain location between adjacent time steps, and is set to 1 h. All types of simulations are briefly summarized in Table 1.

As an example, we use the Amazon region (15°S–5°N, 70°–40°W) as a test bed for the schemes proposed in this study. The simulation period in all experiments is from 1 January to 31 December of 2001. The National Centers for Environmental Prediction–National Center for Atmospheric Research (NCEP–NCAR) reanalysis data are used as a surrogate for the forcing simulated by atmosphere models. Different than the default CLM3 that uses Advanced Very High Resolution Radiometer (AVHRR)-based leaf area index (LAI), the LAI in this study is derived from Mod-

Table 1. Experiment types.

	Equations	Highlights
W05		Account for precipitation subgrid variability alone
EXP1	(1)–(8)	Two treatments based on W05: 1) adjust partition between canopy interception and throughfall within rain-covered area and 2) account for subgrid variability of canopy storage and track relative location of rain
EXP2	(2)–(8)	Same as EXP1 but excluding treatment 1
EXP3	(1)	Same as EXP1 but without treatment 2

erate Resolution Imaging Spectroradiometer (MODIS) observations (Tian et al. 2004). Our analysis focuses on the interception loss and total evapotranspiration (ET), because these two variables are most directly influenced by model parameterization changes presented in this study. The ratio presented here is defined by the yearly mean interception (or evapotranspiration) as a fraction of the yearly mean precipitation.

Table 2 shows the regionally averaged interception loss ratio and the corresponding ET ratio simulated by CLM3 in W05, EXP1, EXP2, and EXP3 with the time steps of 10 min, 20 min, 1 h, and 2 h over the Amazon region. In W05, the interception loss ratio decreases by 80% from 0.46 at 10-min time step to 0.09 at 2-h time step. The corresponding change of the ET ratio is smaller but still significant (40% decrease). It is evident that these two ratios are very sensitive to temporal resolution in W05. In contrast, the new scheme in EXP1 is much more robust in simulating these two ratios. Changing the resolution from 10 min to 2 h reduces the interception loss ratio from 0.3 to 0.23, a reduction of 23%, which is much smaller compared with that in W05. Correspondingly, the ET ratio is reduced by only 11%. Figure 1 shows the interception loss ratio at two different temporal resolutions (i.e., 20 min and 1 h) in W05 and EXP1 and their differences with a 2D contour plot. The 20-min resolution is often used in coupled land–atmosphere models, while 1 h is often used in offline land surface models. The difference in interception loss ratio between the two time steps is above 0.2 for most areas in W05, which is much larger compared with ~0.05–0.075 in EXP1. Taking results from EXP1 as the truth, W05 overestimates interception loss at fine temporal resolutions (10 and 20 min) and underestimates interception loss at coarse temporal resolutions (1 and 2 h), which are consistent with the two problems we identify as major causes for the undesirable sensitivity of the Shuttleworth scheme described in section 2. The reduction of the sensitivity to temporal resolution in EXP1 is attributed to the two treatments in Table 1. The relative importance of the two can be examined by comparing the results of EXP1 with those of EXP2 and EXP3, each of which excludes the treatment targeted to one of the two problems described in section 2.

As shown in Table 2, if results from EXP1 are taken as the ground truth, it is evident that EXP2 underestimates the interception loss at the relatively coarse 1- and 2-h resolutions and EXP3 overestimates them at the fine 10- and 20-min resolutions. Both EXP2 and EXP3 show substantial sensitivity to temporal resolution, and the sensitivity is larger than EXP1 but smaller than W05. The treatment contributing to EXP1's low sensitivity to temporal resolution, which is not included in EXP2, is the adjustment of canopy interception to sustain some wetness in the canopy within the rain-covered area during rainy time steps as described in Eq. (1). As explained earlier, this treatment is targeted to a problem that occurs more frequently at coarse temporal resolution, namely, when the time step is too long, the canopy water storage at its full capacity within the rain-covered area is not enough to sustain the potential evaporation through the time step. When EXP2 excludes this treatment, the canopy interception, and therefore the interception loss, is more severely underestimated under the coarse temporal resolution. As the time step becomes small enough (e.g., 10 min), the in-

Table 2. Regionally averaged interception loss and ET ratios at different temporal resolutions.

	Interception loss ratio				ET ratio			
	10 min	20 min	1 h	2 h	10 min	20 min	1 h	2 h
W05	0.455	0.351	0.165	0.089	0.694	0.625	0.481	0.415
EXP1	0.301	0.272	0.227	0.229	0.589	0.568	0.530	0.523
EXP2	0.296	0.256	0.153	0.089	0.588	0.562	0.485	0.432
EXP3	0.402	0.332	0.237	0.226	0.657	0.609	0.536	0.521

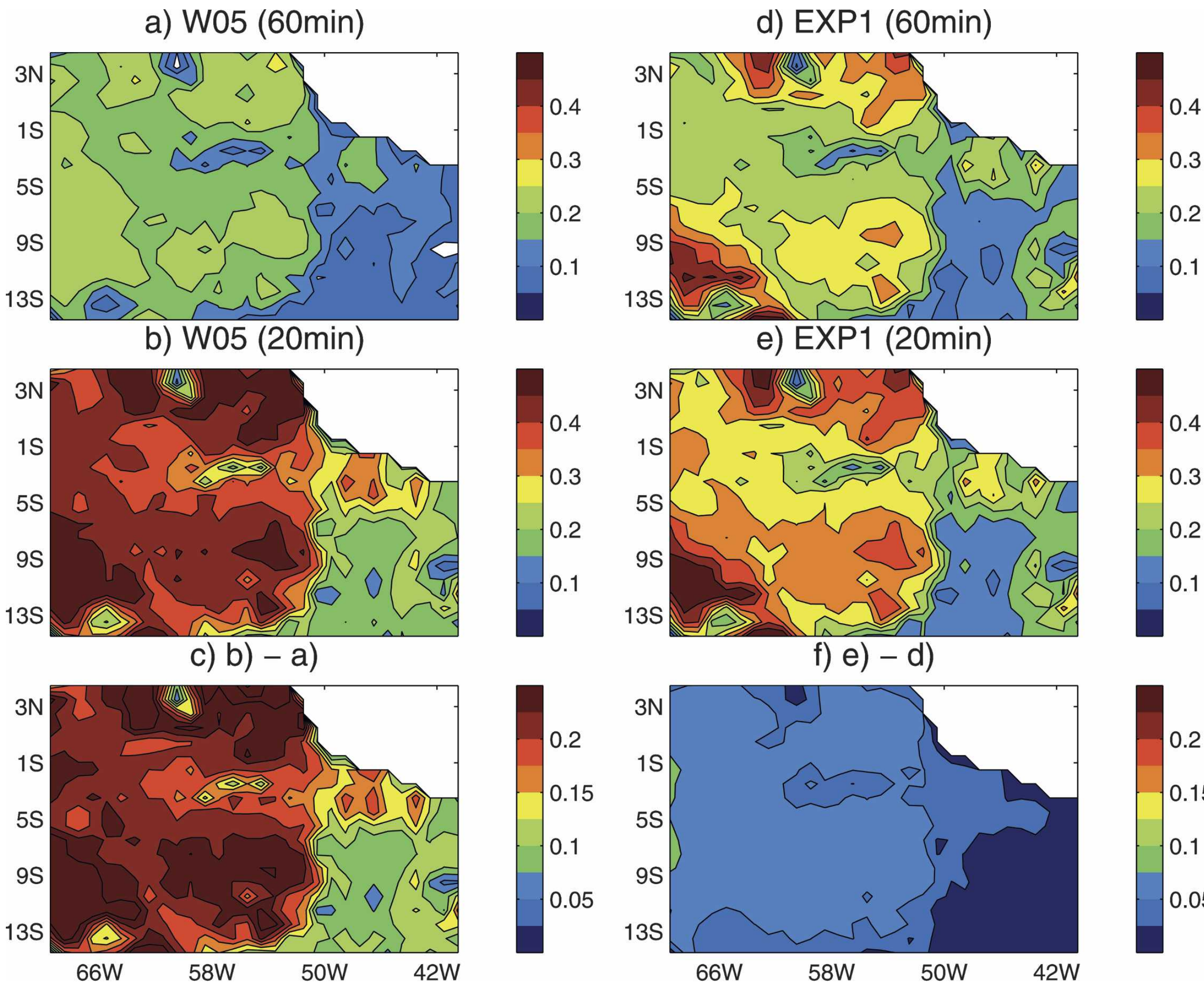

FIG. 1. Interception loss ratio (interception loss as a fraction of precipitation) at different temporal resolutions in W05 and EXP1 and their differences.

terception loss ratio in EXP2 is very close to that in EXP1.

The treatment contributing to EXP1's low sensitivity to temporal resolution, which is excluded from EXP3, concerns how to determine the canopy storage at the beginning of a rainy time step for the rain-covered area. EXP3 redistributes the canopy storage at the beginning of every time step and estimates the canopy maximum infiltration rate I_{max} based on the resulting grid-averaged canopy storage. EXP1, however, tracks the location of rain from one step to the next and estimates I_{max} based on the canopy storage within the rain-covered area at the beginning of every time step. In addition, in EXP1, rain is assumed to fall repeatedly over the same location within a typical convective duration of 1 h and changes location every 1 h (the adopted typical convective rain duration). The uniform redistribution of canopy storage in EXP1 takes place only when the rain first ends. This treatment is most effective when the temporal resolution is small and does not make a difference when the length of the time step is equal to or longer than the typical rain duration. This understanding is confirmed by comparing EXP3 with EXP1; little difference is found in the interception loss ratio between EXP1 and EXP3 at the time steps of 1 and 2 h, while a large difference at the 10- and 20-min temporal resolutions is found.

4. Summary and discussion

This paper presents a robust canopy hydrology scheme in which two physically based treatments are applied to reduce the temporal resolution sensitivity of canopy interception based on our previous work (W05). In this scheme, the canopy interception and the subsequent canopy hydrological processes in the rain-covered area are simulated separately from those in the nonrain area. The scheme tracks the relative location of rain between adjacent time steps by assuming that rainfall falls repeatedly over the same location within a typical convective rain duration and shifts to another location beyond that duration. The canopy maximum infiltration rate is estimated based on the canopy water storage within the rain-covered area. The storage is redistributed to be uniform across the grid cell only when rain first ends at the grid level. In addition, the canopy interception rate is adjusted to ensure that some wetness in the canopy is maintained throughout each rainy time step to reflect the fact that the canopy cannot be completely dry when it rains. When incorporated into CLM3, the scheme performance is fairly stable under different temporal resolutions. Based on the simulations over the Amazon region, interception loss ratio decreases by 23% from 0.3 at 10-min time step to 0.23 at 2-h time step in the new scheme, which is much smaller compared to a decrease of interception loss ratio from 0.45 to 0.09 at the corresponding time steps in W05.

When estimating the canopy maximum infiltration rate, our scheme assumes the beginning canopy storage in each time step is spatially uniform within the rain-covered area. Its spatial variability within the rain-covered area is not considered. This simplification is made based on the fact that after dripping and evaporation during the previous time step, the canopy storage at the beginning of each time step is usually small and much smaller than its holding capacity. A natural question is how much difference it will make if the probability distribution of the beginning canopy storage is considered. To address this question, we assume the beginning canopy storage (S) within the rain-covered area follows a truncated exponential distribution between zero and the canopy holding capacity $f(S)$ and that the precipitation distribution $f(P)$ is independent of $f(S)$ to rederive the estimate of canopy interception as

$$\mathrm{Ic}_{\mathrm{rain}} - \mathrm{Dr}_{\mathrm{rain}} = \frac{P_m}{\mu} - \frac{P_m^2\Delta t\left[\exp\left(-\frac{C}{\mathrm{Sb}_{\mathrm{rain}}}\right) - \exp\left(-\frac{\mu C}{P_m\Delta t}\right)\right]}{\mu^2\mathrm{Sb}_{\mathrm{rain}} - \mu P_m\Delta t}. \tag{9}$$

When $\mathrm{Sb}_{\mathrm{rain}}$ is zero or much smaller than C (which is the case based on numerical modeling results not shown here), Eq. (9) reduces to Eq. (2). Not surprisingly, when an experiment is run that is otherwise the same as EXP1 but with Eq. (2) replaced by Eq. (9), the regionally averaged interception loss ratios are 0.276 and 0.227 at the temporal resolutions of 20 min and 1 h, respectively, which are almost the same as those in EXP1 (0.272 and 0.227, correspondingly). Therefore, once the canopy storage in the rain-covered area is treated separately from that in the nonrain area, further details of the spatial variability of canopy storage within the rain-covered area are no longer critical.

When applied to the Amazon region, the new scheme still overestimates interception loss ratio (Shuttleworth 1988a) by a factor of 1.5–2 or so. This can be due to three possible reasons: first, the water holding capacity of the vegetation (currently 0.1 mm per unit LAI) may be overestimated (Herwitz 1985); second, canopy dripping is assumed to occur only when storage exceeds capacity, while in reality it does occur even if storage is less than capacity (Dolman and Gregory 1992); and third, the measurement conducted in a specific site might not represent the characteristic of large area. However, in this study, the focus is on the physical realism of the parameterization for canopy hydrological processes thus reducing the model sensitivity to temporal resolution instead of nudging the model results one way or the other.

Finally, when implementing the new canopy hydrology scheme into CLM3, we assumed a typical convective rain duration of 1 h based on measurement carried out in the Florida peninsula. This critical characteristic of precipitation necessarily varies from place to place. Precipitation observations that shed light on the duration of convective rain over regions where the scheme is applied will improve the realism of model results. Note that the scheme presented in this study is applied to a convective dominated area, that is, the Amazon basin. For mid- and high-latitude areas where stratiform rain accounts for a substantial portion of total rain, one needs to distinguish between the two types of rain and treat them differently. We are currently working on developing the scheme that treats convective and stratiform rain differently.

Acknowledgments. This study was supported by a NASA Earth System Science Fellowship (NNG05GP38H) (for Mr. Dagang Wang) and Georgia Institute of Technology (NNG04GB89G) (for Dr. Guiling Wang). The authors thank the three anonymous reviewers for their helpful comments.

REFERENCES

Cosgrove, C. M., 1999: Volumetric and spatial dimensions of convective rain events. Ph.D. dissertation, University of Virginia, 115 pp.

Dickinson, R. E., and A. Henderson-Sellers, 1988: Modeling tropical deforestation: A study of GCM land surface parameterizations. *Quart. J. Roy. Meteor. Soc.,* **114,** 439–462.

Dolman, A. J., and D. Gregory, 1992: The parameterization of rainfall interception in GCMs. *Quart. J. Roy. Meteor. Soc.,* **118,** 455–467.

Eltahir, E. A. B., and R. L. Bras, 1993: Estimation of the fractional coverage of rainfall in climate models. *J. Climate,* **6,** 639–644.

Gash, J. H. C., 1979: An analytical model of rainfall interception by forests. *Quart. J. Roy. Meteor. Soc.,* **105,** 43–45.

——, C. R. Lloyd, and G. Lachaud, 1995: Estimating sparse forest rainfall interception with an analytical model. *J. Hydrol.,* **170,** 79–86.

Herwitz, S. R., 1985: Interception storage capacity of tropical rainforest canopy trees. *J. Hydrol.,* **77,** 237–252.

Hörmann, G., A. Branding, T. Clemen, M. Herbst, A. Hinrichs, and F. Thamm, 1996: Calculation and simulation of wind controlled canopy interception of a beech forest in northern Germany. *Agric. For. Meteor.,* **79,** 131–148.

Lean, J., and D. A. Warrilow, 1989: Simulation of the regional climatic impact of Amazon deforestation. *Nature,* **342,** 411–413.

Liang, X., D. P. Lettenmaier, and E. F. Wood, 1996: One-dimensional statistical dynamic representation of subgrid spatial variability of precipitation in the two-layer variable infiltration capacity model. *J. Geophys. Res.,* **101,** 21 403–21 422.

Pitman, A. J., A. Henderson-Sellers, and Z. L. Yang, 1990: Sensitivity of regional climates to localized precipitation in global models. *Nature,* **346,** 734–737.

——, Z. L. Yang, and A. Henderson-Sellers, 1993: Sub-grid scale precipitation in AGCMs: Reassessing the land surface sensitivity using a single column model. *Climate Dyn.,* **9,** 33–41.

Rutter, A. J., K. A. Kershaw, P. C. Robins, and A. J. Morton, 1971: A predictive model of rainfall interception in forests. I: Derivation of the model from observations in a plantation of Corsican pine. *Agric. For. Meteor.,* **9,** 367–384.

——, A. J. Morton, and P. C. Robins, 1975: A predictive model of rainfall interception in forests. II: Generalization of the model and comparison with observations in some coniferous and hardwood stands. *J. Appl. Ecol.,* **12,** 367–380.

Scott, R., R. Koster, D. Entekhabi, and M. Suarez, 1995: Effect of a canopy interception reservoir on hydrological persistence in a general circulation model. *J. Climate,* **8,** 1917–1922.

Shuttleworth, W. J., 1988a: Evaporation from Amazonian rainforest. *Proc. Roy. Soc. London,* **B233,** 321–346.

——, 1988b: Macrohydrology—The new challenge for process hydrology. *J. Hydrol.,* **100,** 31–56.

Tian, Y., and Coauthors, 2004: Comparison of seasonal and spatial variations of LAI/FPAR from MODIS and Common Land Model. *J. Geophys. Res.,* **109,** D01103, doi:10.1029/2003JD003777.

Wang, D. G., G. L. Wang, and E. N. Anagnostou, 2005: Use of satellite-based precipitation observation in improving the parameterization of canopy hydrological processes in land surface models. *J. Hydrometeor.,* **6,** 745–763.

Wang, G. L., and E. A. B. Eltahir, 2000: Impact of rainfall subgrid variability on modeling the biosphere–atmosphere system. *J. Climate,* **13,** 2887–2899.